

Joint geophysical modelling constrained by geological and petrophysical data for assessing the geothermal energy potential of the Romagna and Ferrara folds (RFF), Eastern Po-plain

Basant R.*¹, Tesaro M.¹⁻², Cortassa V.¹, Gola G.³, Nanni T.³, Slupski P.M.⁴, Galgaro A.⁴ & Manzella A.³



1. Dipartimento di matematica, Informatica e Geoscienze, Università di trieste, Italy,

2. Utrecht University, Netherlands

3. Istituto di Geoscienze e Georisorse, CNR, Italy

4. Dipartimento di Geoscienze, Università di Padova, Italy



1. INTRODUCTION

2. GEOPHYSICAL MODELLING WORKFLOW

The InGEO project (Innovation in GEOthermal resources and reserves potential assessment for the decarbonization of power/thermal sectors, www.ingeo.cnr.it), seeks to develop an innovative exploration workflow for integrating geological, geophysical and petrophysical datasets. The aim of this study is to jointly interpret seismic tomography, gravity and well log data in the Romagna and Ferrara Folds (RFF), in order to implement a consistent 3D geophysical model to use as input for the evaluation of geothermal resources

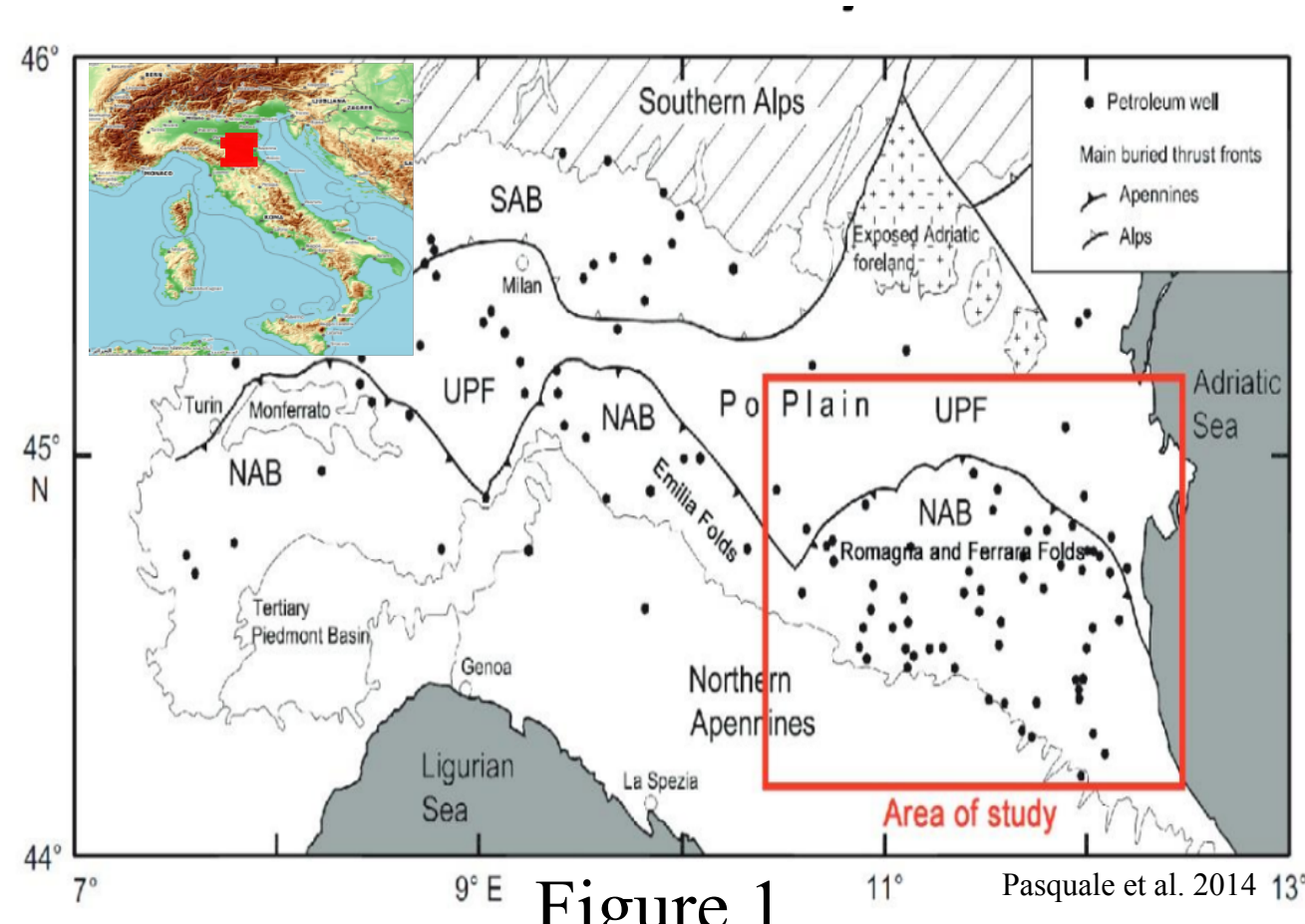


Figure 1

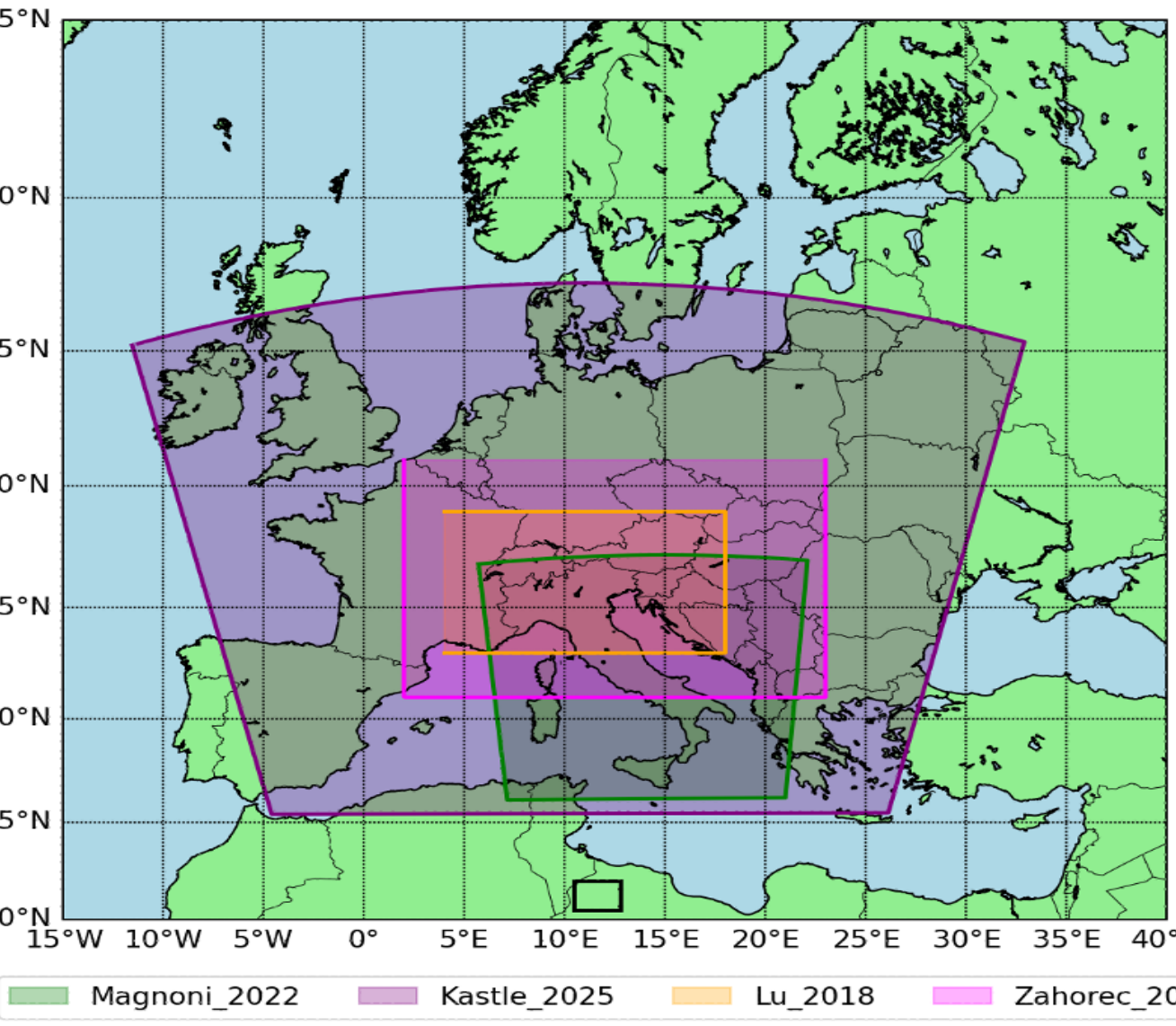


Figure 2

The aim of the geophysical modelling section of the InGEO involves both seismic and gravity modelling. Figure 3 shows the workflow we designed to achieve this aim. The workflow is divided into three main sections: 1) INPUT 2) PROCESSING and 3) OUTPUT. For this study, we utilized only the steps for seismic tomography and gravity analysis. Sonic well logs are utilized in validating our models.

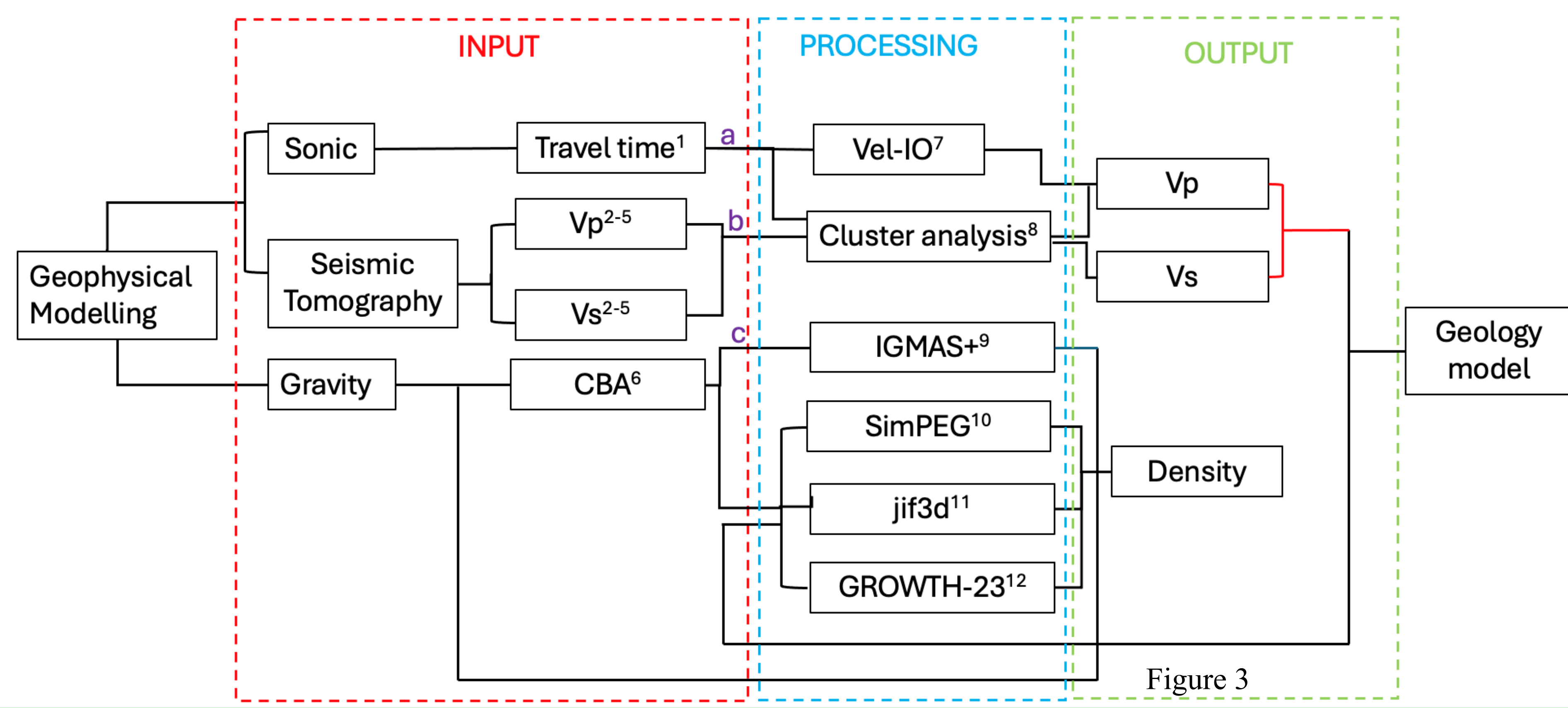


Figure 3

3. RESULTS

4. DISCUSSION

A. Seismic Tomography

Step 1: Interpolation of datasets

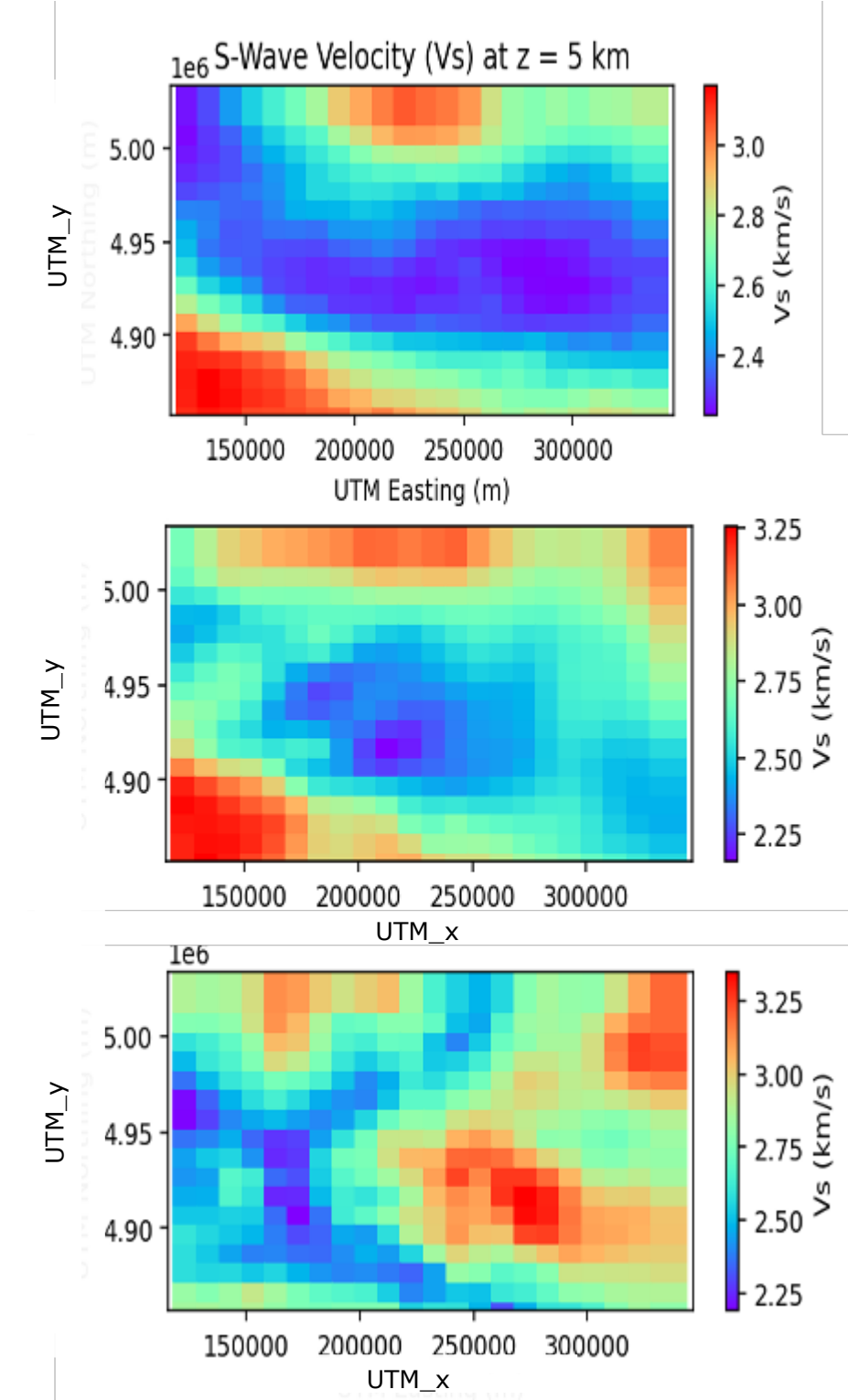


Figure 4

Step 2: Applying clustering algorithm

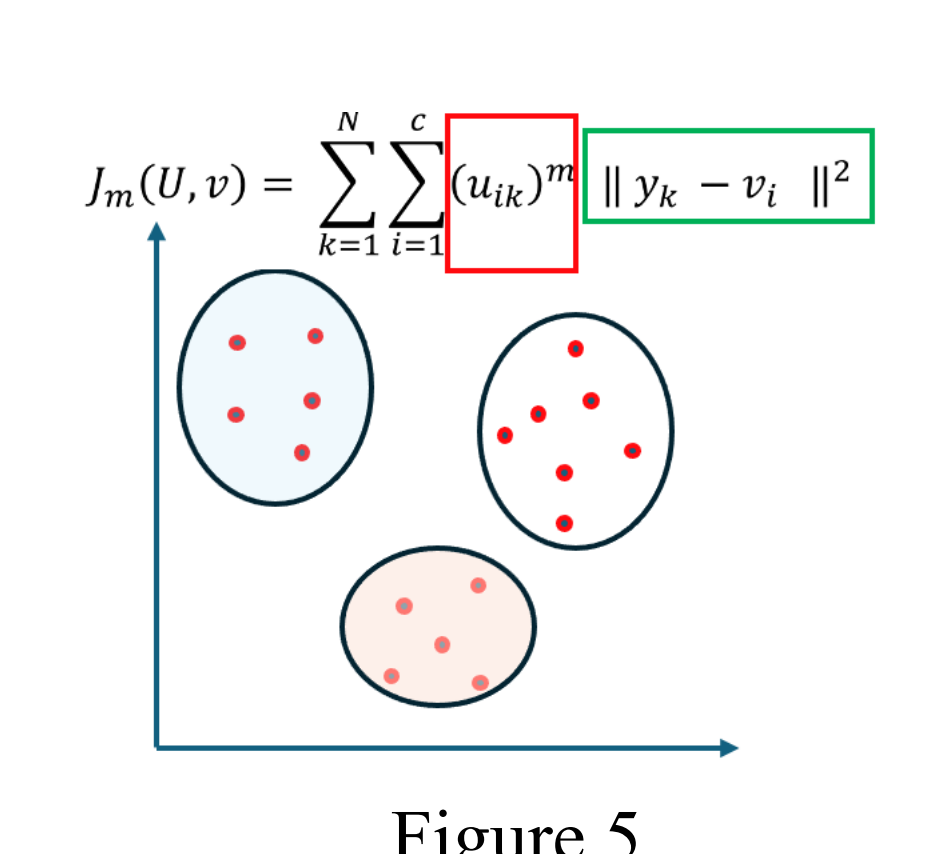


Figure 5

Step 3: Selecting optimal number of clusters

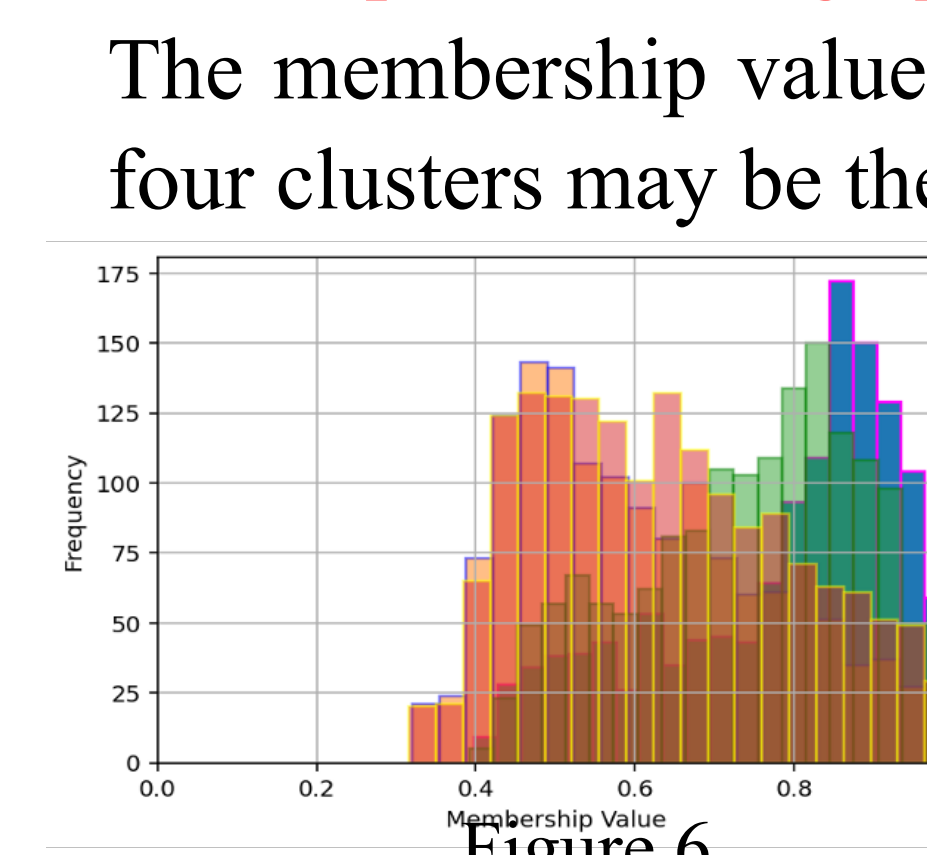


Figure 6

Seismic Tomography models (S-wave) were displayed over the RFF domain. Figure 4 shows a low velocity anomaly over the RFF region. The data were interpolated over a 10 km interval spacing so that each point within the grid was characteristic of a S-wave velocity of each model.

Clustering algorithms can be used to classify similarities amongst datasets. The Fuzzy c-means (FCM) algorithm was used to classify the S-wave seismic tomography models.

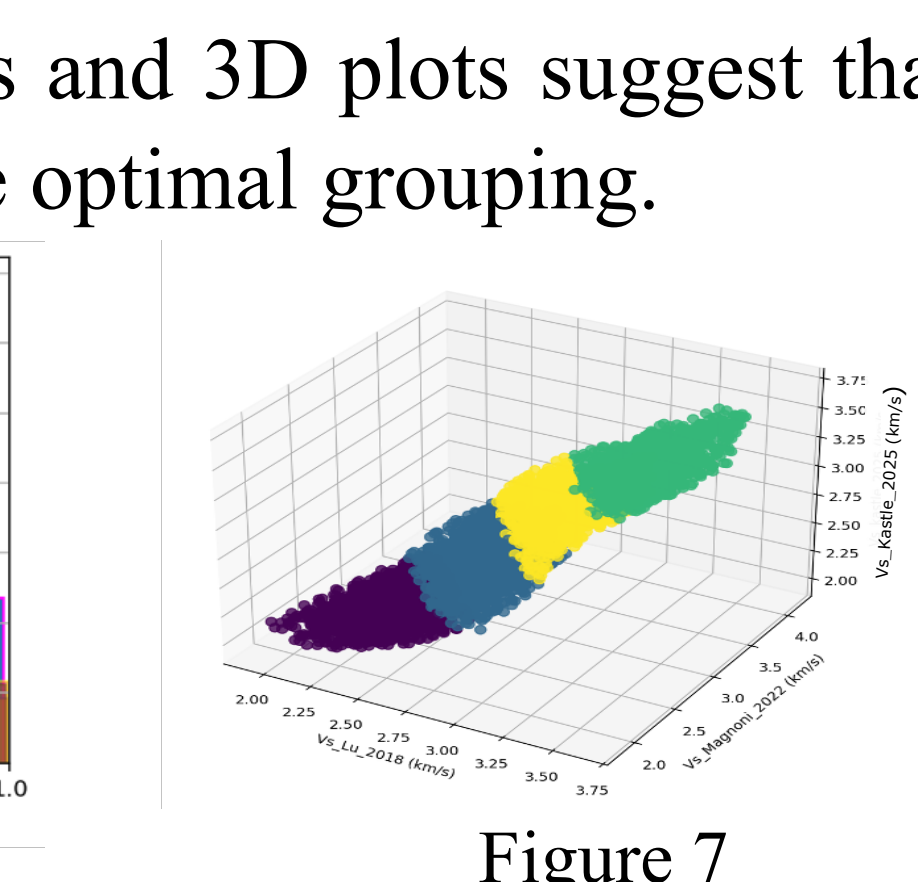


Figure 7

B. Gravity Modelling

Step 1: Gravity residual calculation

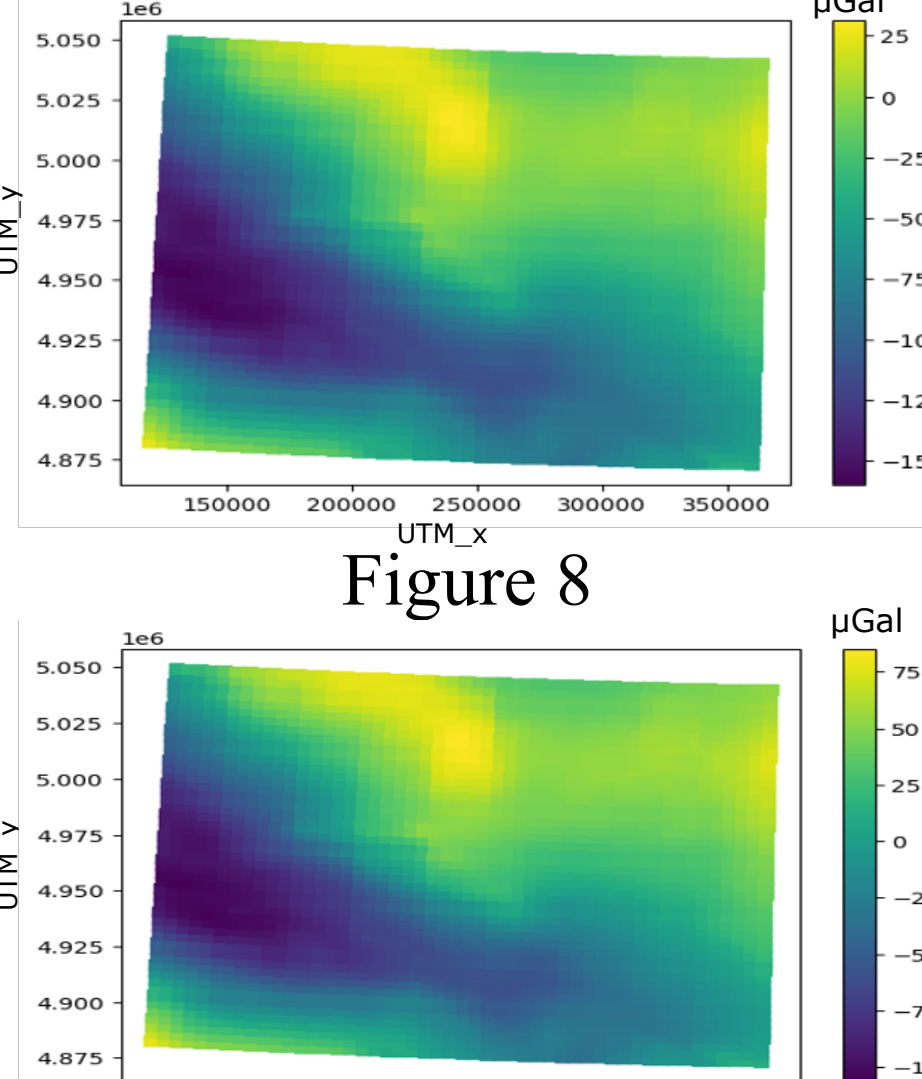


Figure 8

Figure 9

Step 2: Inversion Mesh

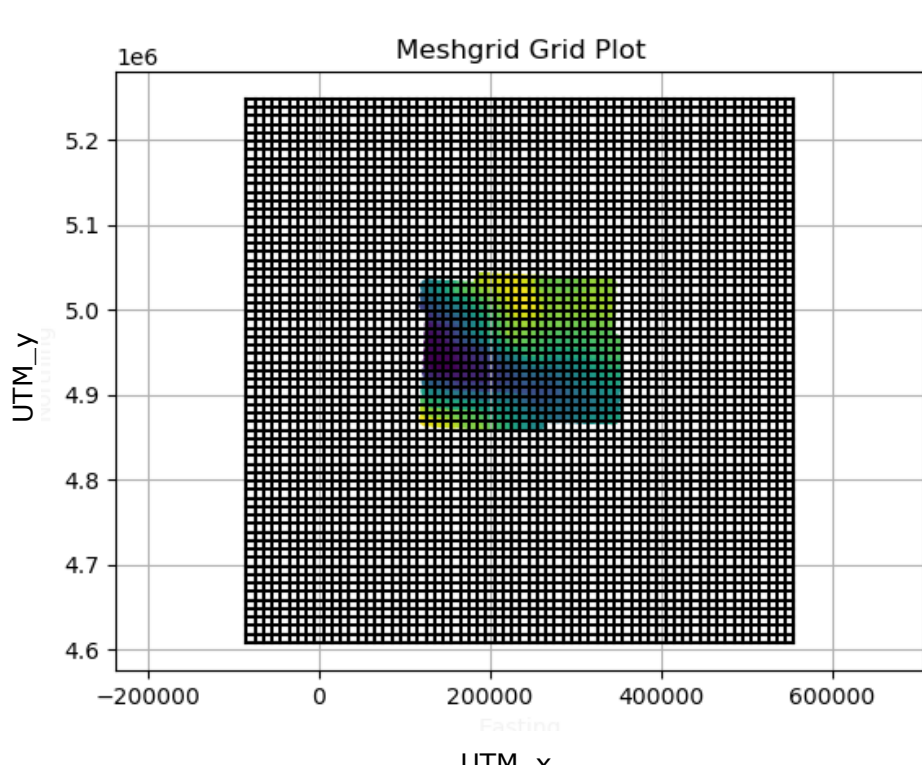


Figure 10

Step 3: Gravity inversion

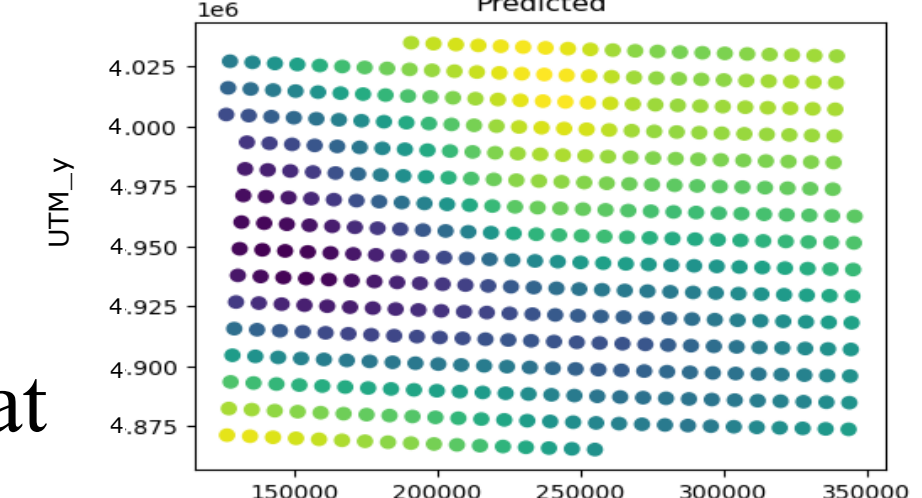


Figure 11

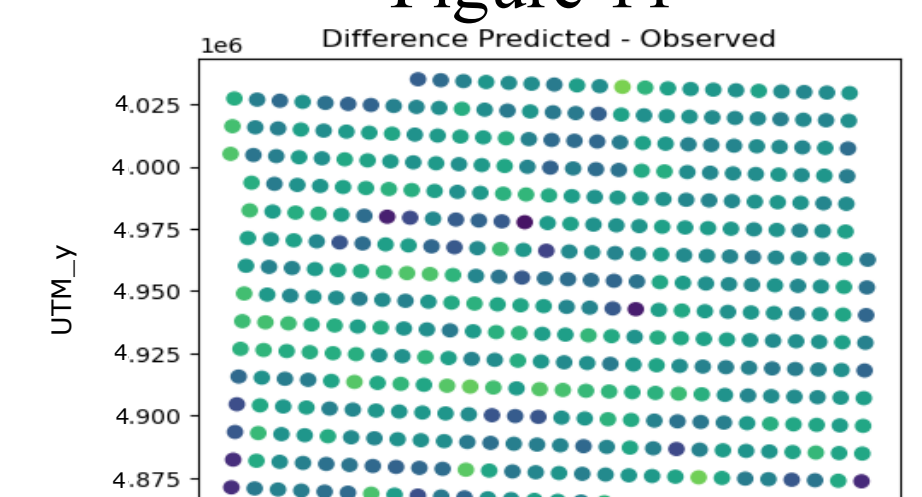


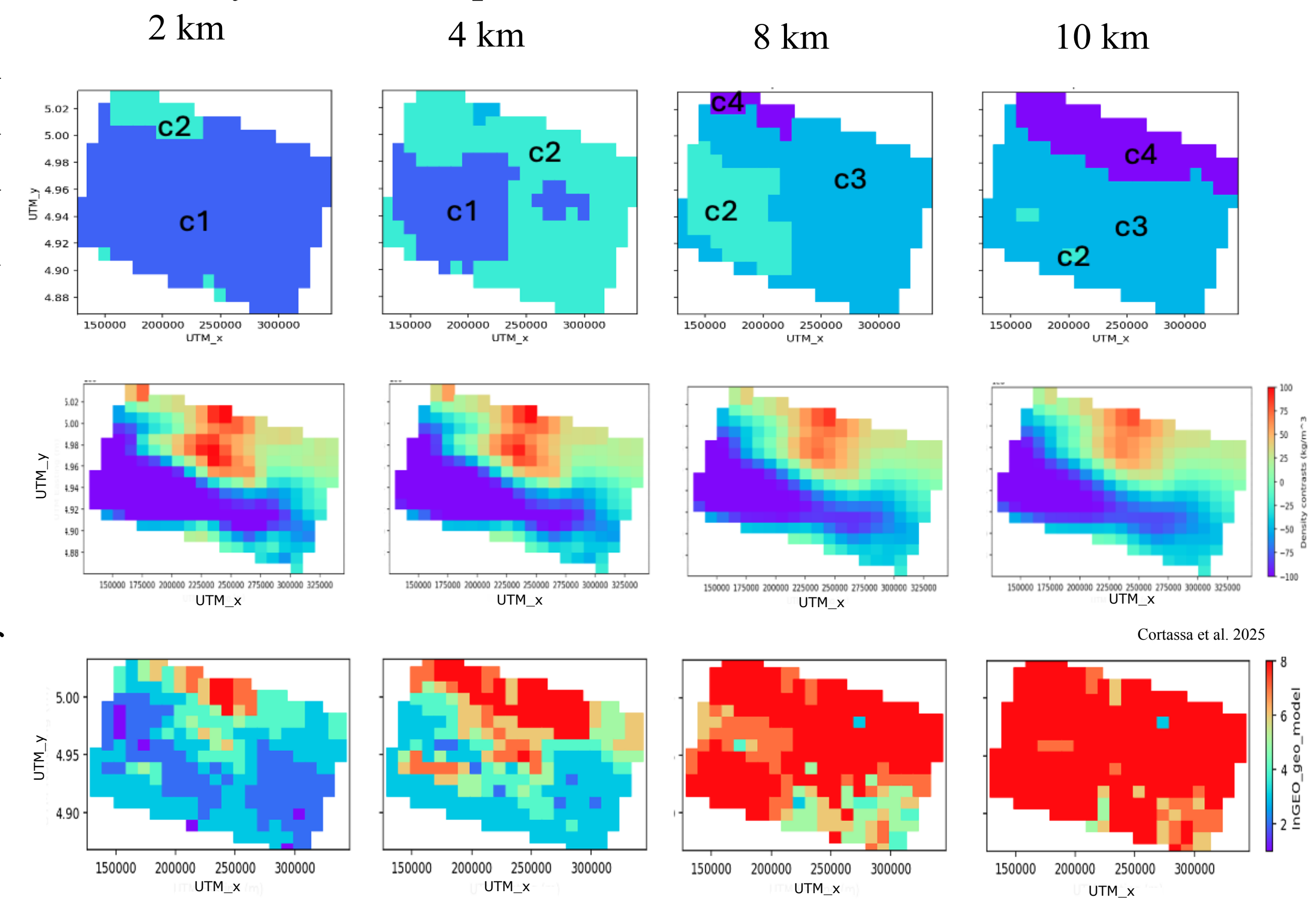
Figure 12

Gravity dataset consisting of land and marine acquisitions over the RFF. The complete Bouguer anomaly (Figure 8) shows a low NW-SE anomaly spatially coincident with the seismic tomography. The residual CBA is shown in Figure 9.

The inversion model was built by a volume discretized in voxels of 64 x 64 x 50. Horizontal resolution was set as 10 km and vertical resolution was set at 1 km respectively.

Figure 11 shows the computed or predicted gravity. Comparison with the observed gravity (Figure 8) shows the NW-SE trending low anomaly. Figure 11 shows the residuals (difference between observed and predicted) are low. RMS = 2.28

The cluster model and density contrasts model highlight increasing S-wave velocity and density contrasts respectively with depth. The main anomalous region include the low velocity anomaly (c1) coincident with the low density anomaly. The geology model and well logs show that this anomaly can be interpreted as Plio-Pleistocene sediments.



1-Quaternary, 2-Plio-Pleistocene, 3-Miocene, 4-Paleogene, 5-Cretaceous, 6-Triassic, 7-Jurassic, 8-Permian

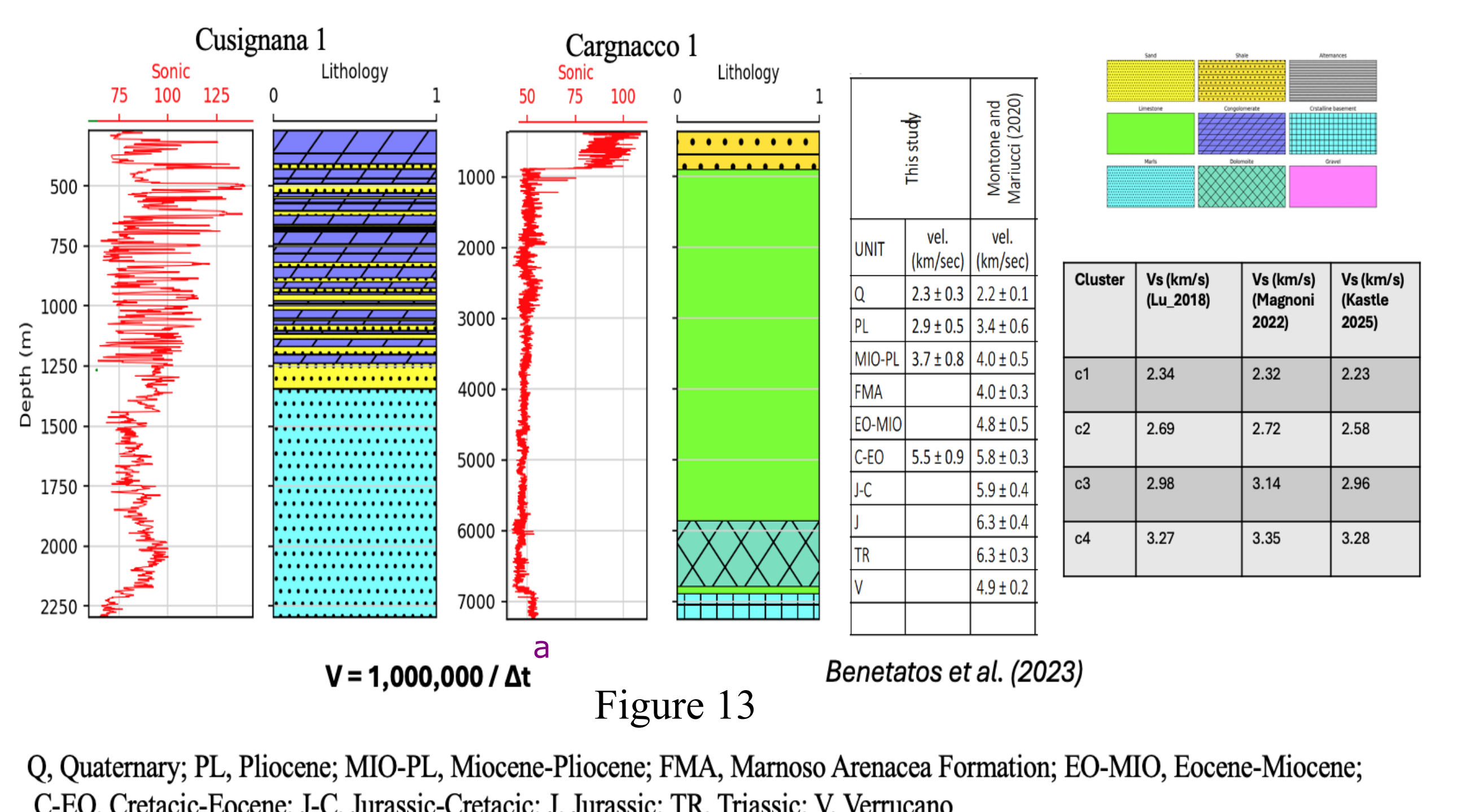


Figure 13

Q, Quaternary; PL, Pliocene; MIO-PL, Miocene-Pliocene; FMA, Marnoso Arenacea Formation; EO-MIO, Eocene-Miocene; C-EO, Cretacic-Eocene; J-C, Jurassic-Cretacic; J, Jurassic; TR, Triassic; V, Verrucano

5. CONCLUSIONS

6. OUTLOOK

1. Three-dimensional modelling and constraint of the anomalous regions in the RFF.
2. Lowest velocity and lowest density interpreted as sediments of the Plio-Pleistocene geological unit.
3. High velocity and high density anomalies interpreted as older geological units.
4. Validation of the cluster and density contrast model with geological model and sonic well logs.

1. Velocity model refinement with sonic well logs using the Vel-IO tool
2. Constraint of gravity inversion using a priori density model from seismic
3. Uncertainty analysis of both seismic and gravity datasets
4. Implementation of a consistent geological/geophysical model to utilize in a numerical model that will characterize the geothermal reservoir potential
5. Working towards a workflow that is reproducible and can be applied to de-risk future geothermal prospects in any region/area.

References

1. J. J. M. P. et al., 2023. Subsurface geological and geophysical data from the Po Plain and the northern Adriatic Sea (northern Italy). Earth System Science Data Discussions, 2023, pp. 1-41.
 2. Kallitri, E.D., Paffrath, M., El-Sharkawy, A. and Alparat, A. 2023. Alpine Crust and Mantle Structure from 3D Monte Carlo Surface and Body-Wave Tomography. Journal of Geophysical Research: Solid Earth, 128(2), p. e2022JB021011.
 3. Magagnoli, F., Casarotti, E., Komarich, D., Di Stefano, R., Cicco, M.G., Tappi, C., Meloni, D., Michelini, A., Porsani, A. and Tromp, J. 2022. Joint tomography of the Italian lithosphere. Communications Earth & Environment, 3(1), p. 69.
 4. Lu, Y., Shieh, L., Paul, A. & Alparat, A. 2019. High-resolution surface wave tomography of the European crust and uppermost mantle from ambient seismic noise. Geophysical Journal International, 214(2), 1136-1150.
 5. Rappos, F., Lo Bae, R., Vandroeck, B.P., Confai, J.M., Erman, C., Barchiesi, P., Podda, S., Eke, T., Vostal-Cevikbilen, S. and Favencchi, M. 2025. 3-D mantle flow and structure of the Mediterranean from combined P-wave and splitting intensity anisotropic tomography. Journal of Geophysical Research: Solid Earth, 130(6), p. e2024JB030853.
 6. Zahorec, P., Pappas, J., Palocz, R., Bost, M., Bortolotti, S., Braunberger, C., Ehlig, J., Gabriel, G., Gout, A., Grand, A. and Götze, H.J. 2021. The first pan-Alpine surface gravity database, a modern compilation of cross-frontiers, Earth Syst. Sci. Data geological modelling workflow. Computers & Geosciences, 99, pp. 171-182.
 7. Bortolotti, S., Bortolotti, R. and Jull, W. 1986. FCM: The fuzzy c-means clustering algorithm. Computers & Geosciences, 10(2-3), pp. 191-194.
 8. S. Götze, H.J., Fiedler, C. and Over, M. 2010. IGMAS: a new 3D Gravity, FTG and Magnetic Modelling Software. In Geoinformatics 2010.
 9. Cocker, R., Kang, S., Heagy, J.J., Palocz, S. and Odenburg, D.W. 2015. SimPEG: An open source framework for simulation and gradient based parameter estimation in geophysical applications. Computers & Geosciences, 85, pp. 142-154.
 10. Camacho, A.G., Vajda, P. and Fernández, J. 2024. GROWTH-23: an integrated code for inversion of complete Bouguer gravity anomaly or temporal gravity changes. Computers & Geosciences, 182, p. 105495.
 11. Mookkamp, M. 2022. Deciphering the state of the lower crust and upper mantle with multi-physics inversion. Geophysical Research Letters
 12. Cortassa, V. et al. 2025. Analysis, interpretation and integration of borehole data and seismic reflection profiles into a 3D Geophysical Model of the Romagna and Ferrara Folds, (Eastern Po Plain) for the evaluation of geothermal resources. In: Congresso congresso SIMP-SGL, Abstract book, Padova, 16-18 September 2025.

Acknowledgements

The InGEO project is part of the PRIN 2022 PNRR initiative and is funded by the European Union's NextGeneration EU program.